Efficient testing of segmented aspherical mirrors by use of a reference plate and computer-generated holograms. II. Case study, error analysis, and experimental validation

Feenix Y. Pan, Jim Burge, Dave Anderson, and Alexander Poleshchuk

Segmented mirrors present unique challenges to fabrication and testing that are absent for monolithic optics. Since traditional asphere tests do not address segmented optics adequately, we validate a previously developed method to test large quantities of segments accurately, quickly, and economically. In this test, the aspheric shape of each segment is controlled to high accuracy by use of computer-generated holograms, and the radius of curvature is tightly controlled by use of the reference plate. In an adjoining paper [Appl Opt **43,** 5303 (2004)] we developed the theory for this test, and now we present a complete system design and optimization for measuring the 1.4-m segments from a 30-m F/1 primary. A complete tolerance analysis predicts a test accuracy of 4.8-nm rms surface and excellent accuracy for controlling the geometry of the segment. In addition, a laboratory demonstration using 30-cm optics is presented that demonstrated 3.9-nm rms surface accuracy. © 2004 Optical Society of America

OCIS codes: 220.4840, 120.3940, 220.0220.

1. Introduction

Giant primary mirrors are now being designed for ground- and space-based telescopes. As the mirrors get larger, telescope designers must use a mosaic of smaller elements to create the effect of a single continuous mirror. The twin 10-m Keck Telescopes on Mauna Kea in Hawaii are the best-known examples of this segmented-optics technology.[1]

The production of mirror segments has several unique requirements[2,3]: (a) the relative radii of curvatures (ROC) need to be matched to an interferometric tolerance, (b) per-segment test and manufacturing time must be minimized to meet the drastic increase in number of segments needed for giant mirrors, and (c) alignment accuracy must be tightened to ensure over system performance will not degrade owing to segmentation. Traditional aspherical tests fail to address the requirements of segmented optics; they have no built-in mechanism for establishing relative ROC to an interferometric accuracy, and they do not readily provide a reference for maintaining alignment. In earlier research,[3,4] we introduce a testing technique that addresses all of these pitfalls. This method uses computer-generated holograms (CGH) for testing large quantities of off-axis segments.

In this paper, we briefly revisit the theory of operation in Section 2, and in Section 3 we present a complete system design and optimization for testing 634 segments from a 30-m F/1 primary.[3] In Section 4 we show the complete tolerance analysis and finally, in Section 5, we present results from a laboratory demonstration validating this new method.

2. Theory of Operation

The new test measures off-axis aspherical mirror segments by use of a CGH and a test plate. It compares a concave segment to a matching-in-size convex spherical reference surface of the test plate. CGHs are used to compensate the aspherical departure of the segments from the spherical reference surface.

F. Y. Pan co-founded Door-2-Math, P. O. Box 87334, Tucson, Arizona 85754. J. Burge (jburge@optics.arizona.edu) is with the Optical Science Center, University of Arizona, Tucson, Arizona 85721. D. Anderson is with Rayleigh Optical Corporation, 3720 Commerce Drive #1112, Baltimore, Maryland 21227. A. Poleshchuk is with the Institute of Automation and Electrometry, Russia Academy of Sciences, Novosibirsk, Russia.

Received 29 August 2003; revised manuscript received 5 June 2004; accepted 15 June 2004.

0003-6935/04/285313-10$15.00/0

© 2004 Optical Society of America

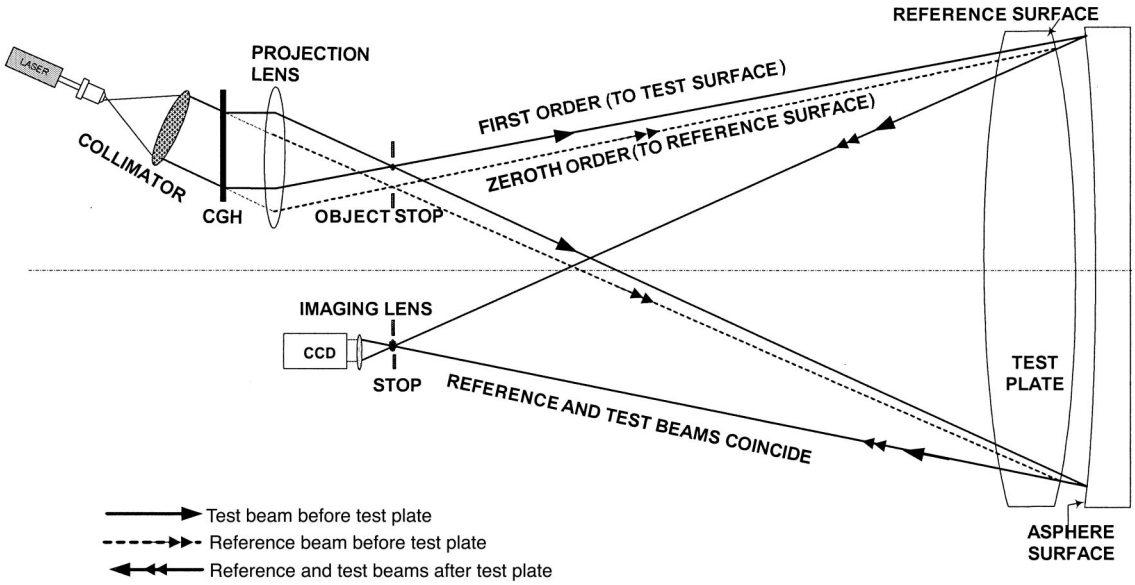

Fig. 1. New test comparing a concave segment with a convex spherical reference surface of the test plate whose size matches that of the mirror segment. CGHs are used to compensate any aspherical departure of the segment from the spherical reference surface. The test plate reference surface is spherical.

The test plate reference surface is chosen to be spherical so it can be cost-effectively manufactured to high accuracy. This reference surface is the only high-quality surface required for the test. The test has a near-common path configuration where test and reference beams travel nearly the same optical path. Figure 1 illustrates how this method works, and it is described completely in the adjoining paper.[4]

3. Case Study

To illustrate the system design and optimization processes described in the adjoining paper we describe a case study for testing a paraboloidal F/1 30-m Giant Segmented Mirror Telescope concept that is currently being studied by the National Optical Astronomy Observatory (NOAO).[5] We developed the test for measuring all 618 of the 1.34-m (point-to-point dimension) hexagonal segments. Since hexagons have six folds of symmetry, only 103 holograms are needed to test all segments. Both the system design and the tolerance analysis given here are from a complete design study performed for NOAO.[6]

We optimized the ROC of the reference side of the test plated to be 60.9203 m (Figs. 2 and 3). This yields a viewing distance of 7.792 m, which does not cause a significant aberration in the illumination. (This viewing distance could be decreased if the ROC of the illumination side is reduced and the surface is made into an asphere.) Because this surface is a common path in the system, the slope errors as large as $2\lambda/\mathrm{cm}$ cause a surface measurement error of only 0.003λ. Table 1 summarizes the three system parameters.

4. Alignment and Error Analysis

The error analysis is divided in two categories—figure errors and errors in the definition of the segment location and rotation with respect to the parent primary. Owing to its large aspherical departure, the tolerance on the farthest-out segment is the tightest, so analysis is performed only for T13, the most difficult segment. The test was designed to meet the necessary requirements for this most severe segment and is over-designed for all other segments. The

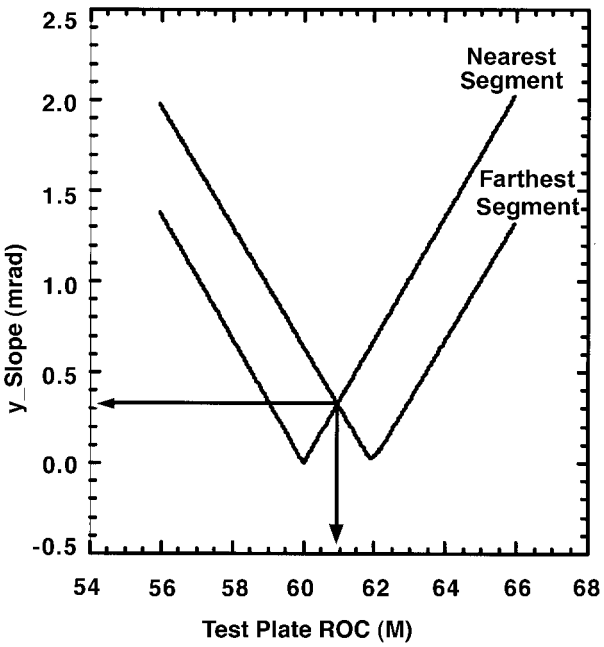

Fig. 2. Optimization of the reference ROC. A ROC of 60.920 m is optimal, because it minimizes the tangential slope. (*y* slope) for the extreme segments. Both inner and outer segments have a slope variation of 0.351 mrad; therefore the nominal tilt in the test is three times this, or 1.05 mrad.

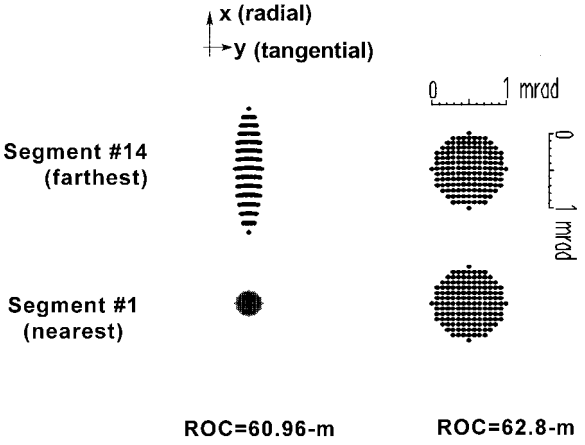

Fig. 3. Spot diagrams for the closest and furthest segments when the reference ROC is 60.96 and 62.8 m, respectively. Two segments of the y slope match for a ROC of 60.96 m, and the x slope matches at a ROC of 62.8 m, but the x slope has a smaller value and is thus used to determine the system parameter reference ROC.

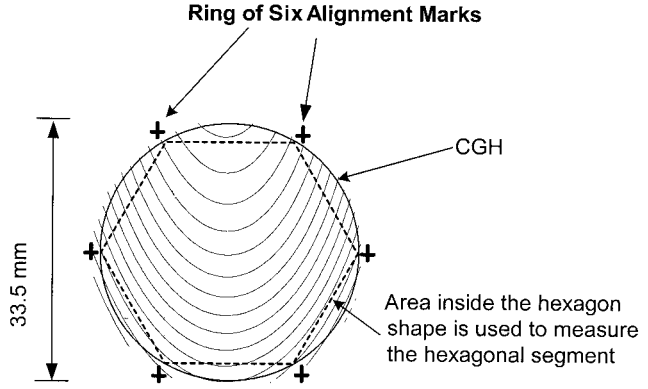

Fig. 4. Ring of six alignment marks etched around the hologram to aid the alignment. This is imaged onto the test plate.

results indicate that the test achieves excellent accuracy for controlling both figure errors and a segment position that utilizes the alignment fiducials.

A. Alignment Fiducials

Accurate axis location is achieved by implementing alignment marks on the CGH directly (Fig. 4) and imaged outside the segment under test. The position of the projected alignment marks will be measured using either a CCD camera or a loupe. The camera or loupe would be aligned with the projected image, and then its position relative to a reference datum would be measured. The distance from this datum to a reference surface on the segments would be controlled to maintain the mechanical alignment of the segment to the optical reference.

B. Figure Error

The figure error described here is defined as a shape error that has a higher spatial frequency than that caused by a misalignment of the segment. Several different components contributing to this error are:

- Wave-front error caused by hologram fabrication inaccuracy.
- Wave-front error caused by errors in the projection optics, which distort the projected images of the hologram.
- Slope errors in the system, typically from refractive-index variations in the test plate, coupled with the slope differences between the two beams.
- Mapping errors that limit the ability to completely back errors out, even if they are known.

Summarized in Table 2 and Fig. 5 is the contribution of each type of errors to a total of 4.8-nm rms surface error in measurement. The error from the hologram fabrication is calculated based on a nominal period of 15-μm spacing and an electron-beam lithography accuracy of 0.125 μm: 0.125/15 or 0.0083λ rms wave-front error. Any surface or refractive-index variation in the hologram substrate does not contribute to the total wave-front error, since the test and the reference beams are a common path at the hologram.

Test plate inhomogeneity and the reference surface affect the test because the incident beams are not a completely common path. For this test, we use 1152λ of tilt across a 1.33-m diameter. This causes 72.6-μm shifts between the two beams at the reference surface. For surface errors with a slope of 2λ/cm, this introduces an error of 0.003 λ. If we assume refractive index variation of 1×10^{-6}, with spatial variation of four cycles across the test plate diameter, the transmitted wave front would have 0.3λ/cm slopes. Since only the test beam goes through the

Table 1. Summary of the System Parameters

System Parameters	Value	Note
Reference Surface ROC (Fig. 2)	60.9 m (convex)	tangential slope,[a] e_y = 0.351 mrad
Illumination Surface ROC	7.8 m (convex)	diffraction-limited spot sizespherical aberration blurred spot size = 15.8%
System Magnification	40×	give hologram size of 33.5 mm in diameter with 15-μm nominal spacing[b]

[a]for the farthest-out segment (Fig. 3).
[b]If these holograms are made onto a 150 mm × 150 mm substrate, we estimate that to test all 103 optically unique segments with six substrates would cost a total of under $45,000.

Table 2. Figure Error Budget for Test of the T13 Segment (the Most Difficult)[a]

Effect	Magnitude	rms Wave-front Error (λ)	rms Surface Figure Error (nm)
CGH fabrication errors	0.125 μm	0.0083	2.63
Projection optics	Table 3	0.0089	2.82
Test plate inhomogeneity	±0.15 mrad	0.0003	0.94
Test plate illumination surface	2 fringes/cm	0.003	0.70
Reference surface figure	Table 4	0.0083	2.63
Segment alignment & test error	Table 5	0.0030	0.95
Root Sum Squared		0.015	4.76

[a]Derivation for all terms is given.

small air gap, it experiences a small net shear difference of 10 μm, which causes 0.0003λ error in the test.

The error budget for the projection optics is more complicated and is determined by direct simulation through a multistep process. To the first order, errors in the projection optics do not affect the test accuracy since both wave fronts go through the projection optics together. In reality, there is a small shear between the two beams in the optical space between the hologram where the two beams separate and the test plate where the two beams are recombined. Table 3, where the effect of projection optics errors is tabulated, is generated by a three-step process. First perturbing each entry the appropriate amount, then realigning the system by use of simulated fiducials, and finally directly comparing the test wave front to the reference wave front. Segment misalignment and error in segment ROC obtained from the previous step is retained and separated from the figure error. The projection system designed for this particular test system has magnification of 40 × and consists of two lenses. Perturbed elements for each lens include two radii of curvatures, two surface figures, inhomogeneity, a wedge angle, and lens position errors such as decenter and tilt. Also included among the perturbed elements are the position of the hologram, the ROC and the wedge of the reference surface, and the thickness and the refractive index of the test plate.

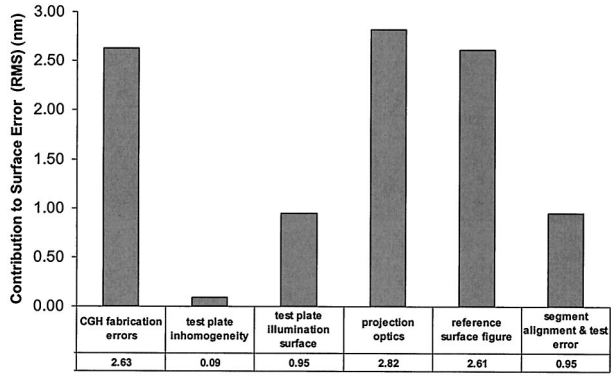

Fig. 5. Five error sources contributing to a total of 4.85-nm uncertainty in surface figure measurement.

The last main error source that contributes to the overall figure error involves the calibration of the reference surface. Before the aspheric segment can be measured, the reference surface of the test plate must be calibrated using a concave reference sphere (RS). This sequence is depicted in Fig. 6. Multiple errors are accumulated through this process. Start with the calibration of the reference sphere. Measurement of RS is accurate to 0.003λ rms by use of a direct shifting interferometer. In addition to this error, there is a limit to how accurately we can remove the errors from the RS measurement out of the reference surface measurement. This inability to completely back out the error introduces approximately 0.0058λ rms wave-front uncertainty if we assume that RS has surface slope of 0.02λ/cm and a mapping error of 2.5 mm. Table 4 summarizes the error budget for measuring the figure from the test plate's reference surface and the RS.

We require tight control on the magnification of the CGH to the test plate. Our alignment procedure uses fiducial marks from the CGH to act as a reference. We envision a ring of six alignment marks fabricated on the same substrate outside the hologram. The FWHM for each mark is ~200 μm at the mirror segment. The spacing of the test plate to the projection lenses will be adjusted to position the fiducial marks with the correct spacing. We assume 0.1-mm accuracy for determining the position of each of the six images 1340 mm apart. Taking averaging into account, our ability to determine scale will be limited to 31 parts per million (0.1 mm/$\sqrt{6}$/1340 mm). The test errors due to this scale effect are simulated and show up in Table 5.

C. Uncertainty in Segment Location

Following the same analysis process, the accuracy of determining the segment location is summarized in Tables 6 and 7. The test is expected to position the segment within ±0.106 mm (radially) and ±0.006 deg (rotationally) and match the ROC to within ±0.39 mm (±24.1-nm surface sag). The equivalent rms wave-front errors corresponding to these alignment errors are summarized in Table 8.

Table 3. Tolerance Analysis for the Projection Optics Used in the NOAO Computer Model[a]

Parameter	Value	Tolerance	Units	Δr (mm)	Δx (mm)	$\Delta\theta$ (deg)	rms WF (λ)
Laser beam		1 wv	wv PV	0.0000	0.0000	0.0000	0.0023
		0.007	deg	−0.0153	−0.0278	0.0000	0.0015
CGH							
Decenter		0.01	mm	0.1847	0.0372	−0.0004	0.0009
Tilt		0.005	mm	0.2041	0.0379	−0.0003	0.0009
Rotation		0.002	deg	0.0040	0.0005	0.0020	0.0008
CGH–L1 spacing	259.9157	0.01	mm	−0.0882	0.0014	0.0000	0.0010
Lens 1							
R1	inf	0.05	mm	0.0000	0.0000	0.0000	0.0001
Center thickness	20	0.01	mm	−0.0541	0.0014	0.0000	0.0007
R2	−126.6618	0.002	mm	0.0781	0.0021	0.0000	0.0008
Index		0.00001		0.01910	−0.00011	−0.00001	0.0013
Surface 1	surf PV	0.125	wave	−0.0063	−0.0005	0.0000	0.0011
Surface 2	surf PV	0.0125	wave	−0.0166	0.0010	−0.0001	0.0009
Inhomogeneity	PV	2.00E-06	–	–	–	–	0.0001
Decenter		0.005	mm	−0.1028	−0.0042	0.0001	0.0012
Tilt	per 100 mm	0.005	mm	0.0054	0.0002	−0.0001	0.0008
Wedge	per 100 mm	0.005	mm	−0.0624	−0.0017	0.0018	0.0018
L1–L2 spacing	94.9862	0.005	mm	−0.0476	−0.0010	0.0002	0.0008
Lens 2							0.0000
R1	−41.21586	0.005	mm	0.0000	0.0031	−0.0001	0.0017
Center thickness	20	0.005	mm	−0.0323	0.0068	−0.0002	0.0002
R2	−49.20629	0.005	mm	0.0197	0.0036	0.0000	0.0015
Index		0.00001					0.0000
Surface 1	surf PV	0.125	wave	−0.0140	0.0018	−0.0002	0.0009
Surface 2	surf PV	0.125	wave	−0.0001	0.0039	−0.0001	0.0013
Inhomogeneity	PV	2.00E-06	–	–	–	–	0.0003
Decenter		0.01	mm	0.0175	−0.0024	0.0000	0.0010
Tilt	per 200 mm	0.01	mm	0.0087	−0.0269	0.0000	0.0024
Wedge	per 200 mm	0.005	mm	−0.0708	−0.0023	0.0021	0.0018
Test Plate							
R1	7791.8688	11.7	mm	0.0175	−0.0006	0.0000	0.0020
Thickness		5	mm	0.0024	0.0000	0.0000	0.0008
Wedge	per 1340 mm	2	mm	0.0010	0.0300	0.0020	0.0060
Root Sum Squared				0.3429	0.0073	0.0040	0.0089

[a]PV, peak-to-valley; WF, wave front; wv, wave at 633 nm.

5. Experimental Validation

The CGH testing method described in Section 2 was validated in a laboratory where a planoconvex test plate was used to measure a concave sphere of known surface quality. A CGH was designed and used in the same manner as the asphere test, but the pattern corresponded to the testing of a sphere. This changes very little in the test sensitivity, as a large tilt carrier always dominates the hologram and its sensitivity.

A. Optical Configuration and Results

The optical system that we used to validate the computer models for the test design and the error analysis included the following:

1. Matching 30-cm test plate and test sphere.
2. A hologram of 20 mm in diameter consisting of chrome patterns written onto flat-glass substrates with nominal line spacing of 15 μm.
3. An off-the-shelf biconvex lens $F = 200$ mm (as the projection system).
4. An off-the-shelf planoconcave lens $F = 50.2$ mm (as the imaging system).

Phase shifting was done by translating the test sphere, and this movement is accomplished by positioning three piezoelectric transducers on the back of the test surface.

A sample CGH used for the test is shown in Fig. 7 (magnified 10x, or every line represents 10λ optical path difference). Clearly, the dominating term is the carrier tilt fringe. A sample interferogram is shown in Fig. 8, and the correspnding surface map from the raw data is shown in Fig. 9.

In this experiment, we designed a system for the CGH test and devised a traditional method to measure the same test surface in the same setup without using the hologram. The new method uses both first and zeroth diffraction orders, whereas the traditional method compares the reference surface directly with the test surface, with no CGH. We then added the hologram to the design and built the setup in the

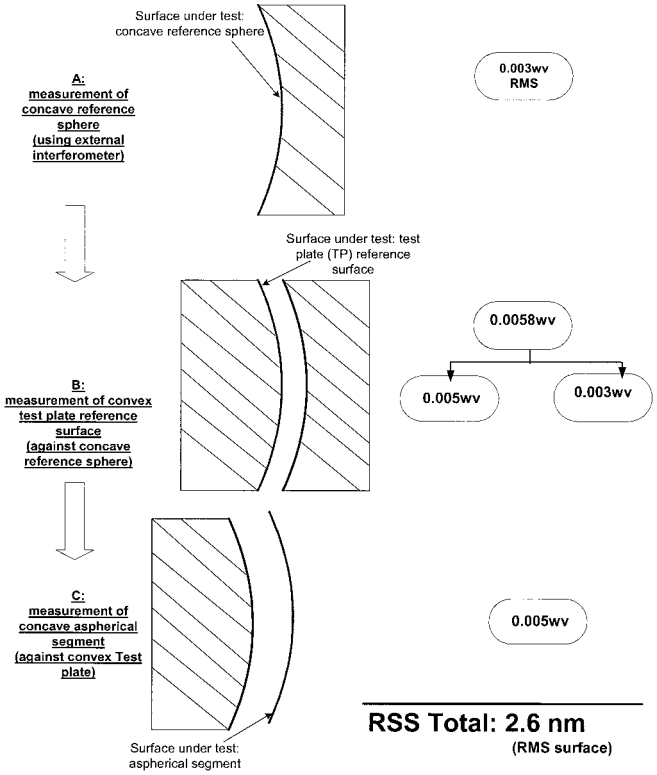

Fig. 6. Error accumulated through calibration of reference sphere and test plate reference surface.

laboratory. The as-built system departed slightly from the nominal design, so both measurements needed a small correction. For the validation, we modeled the laboratory setup in a computer simulation and backed out the residual effect.

The test sphere was measured with the new method and a traditional method. For the traditional method, we used only the zeroth order of the CGH in the same test setup (which is equivalent to not using CGH). Both were corrected with as-built data. Figure 10 shows the results from these two methods. Note that these results are the average of many measurements. This is because individual measurements of the test have smaller random errors that are caused by environmental and/or electronic noises. Since these noises are small in amplitude and are assumed to be uncorrelated, the average of measurements reduces the effect of these noises on the measurement to a negligible level, according to

$$\overline{N} \approx \frac{1}{\sqrt{M}}(n_i) \tag{1}$$

where N is the final noise in the averaged measurement result, M is the number of measurements, and n_i is the individual noise in the ith measurement.

A direct subtraction of the two measurements gives a difference of 0.0116λ rms wave front. This result

Table 4. Error Budget for Measuring Figure from the Test Plate and the Reference Sphere

Effect	Wave-front Error (λ rms)	Figure Error (nm rms)
Measurement of concave reference by use of interferometer	0.003	0.95
Effect of distortion backing out interferometer errors	0.005	1.58
Measurement of convex test plate	0.003	0.95
Effect of distortion backing out reference sphere errors	0.005	1.58
Root sum squared	0.00825	2.61

Table 5. Error Budget for Measuring Surface Figure from the Test Plate and the Reference Sphere

Effect	Magnitude	Surface Figure (λ rms)	Figure (nm rms)
Interferometric measurement	0.003	0.003	0.95
Alignment to fiducials-coupled through magnification effect	6 @ 0.1mm	0.0003	0.10
Root Sum Squared		0.0030	0.95

Table 6. Error Budget for Position and Angle for the T13 Segment Test (the Farthest-out Segment)

Effect	Magnitude	Segment Position Δx (mm)	Segment rotation Δθ (deg)
CGH fabrication errors	0.125 um	0.003	0.0002
Projection optics	Table A3	0.073	0.0040
Alignment to fiducials, coupled by scale effect	6 @ 0.1 mm	0.002	1.4E-05
Alignment to fiducials, direct effect	6 @ 0.1 mm	0.058	0.0035
Mechanical measurements	0.05 mm	0.05	0.0032
Root Sum Squared		0.106	0.006

Table 7. Error Budget for ROC Matching for the T13 Segment Test (the Most Extreme)

Effect	Magnitude	Δsag (nm), ROC Matching	ΔR (mm), ROC Matching
Projection optics	Table 3A	21.38	0.34
Alignment to fiducials, coupled through scale effect	6 @ 0.1 mm	10.54	0.17
Mechanical measurements	0.05 mm	3.12	0.05
Root Sum Squared		24.0	0.39

Table 8. Test Accuracy for the Most Severe Segment

Parameter	Expected Accuracy	Equivalent rms Wave-front Error (nm)
Surface irregularity	4.8 nm	9.6
Relative ROC matching	± 0.39 mm (± 24.1 nm sag)	13.9
Segment radial position	± 0.106 mm	2.9
Orientation of segment	± 0.006 deg (0.105 mrad)	10.86

is consistent with the expected error 0.0124 λ rms wave front, detailed in Section 5.B. This validates the computer model used for the tolerance analysis very well. In addition, tolerance analysis shows that instead of the use of an off-the-shelf BK7 lens as the projection system, the measurement accuracy can be improved to 0.0056λ rms wave front if the quality of the projection lens can be improved from λ/4 peak-to-valley (PV) surface to λ/8 PV surface. One last noteworthy point is that this experiment validation only serves as "proof of concept" and was completed without the aid of alignment fiducial marks that were to be etched on the CGH. Fiducial marks allow for an accurate registration of the CGH with respect to the position of the surface under test. In the absence of these marks, the only aberration we could visually remove from the interferogram is the defocus (by nulling out the interferogram). The result shown in Fig. 12 predicts that if residual coma and astigmatism can be taken out of the measurement, the net accuracy would on the order of 0.007λ rms wave front.

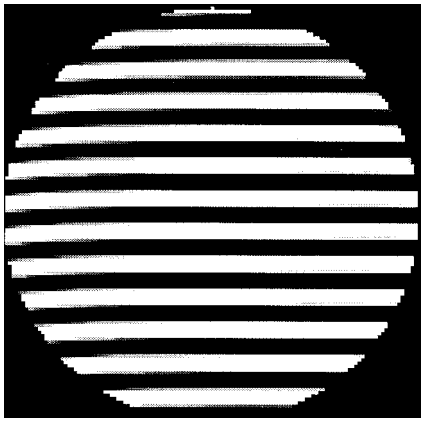

Fig. 7. Sample CGH (plotted here with each fringe representing a 10-λ optical path difference) used to validate the new test method. Here, a 30-cm convex sphere with a known surface quality was tested by use of a CGH and a 30-cm test plate. The CGH was designed and used in the same manner as the testing of an asphere. The dominating feature on the CGH is a large tilt carrier fringes (126 λ across the 20-mm hologram), so test sensitivity is the same as that of testing an asphere.

B. Error Analysis and Lessons Learned

Detailed error analysis was performed on the computer model of the system to obtain the theoretical accuracy of the test. From Fig. 13 and Table 9 we see that three dominating errors are from the surface irregularities of the projection lens and from the surface slope of the illumination surface of the test plate.

One important lesson learned form this experiment is that coaxial setup is a very effective way to improve the test accuracy. From Fig. 13 we see that three dominating errors are from the surface irregularities of the projection lens and from the surface slope of the illumination surface of the test plate. The first two (from the same lens) are relatively inexpensive to correct, as the size of the projection lens is only

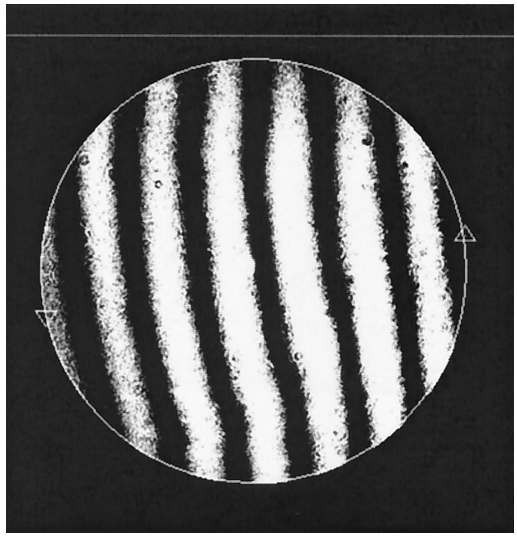

Fig. 8. Sample interferogram showing excellent contrast.

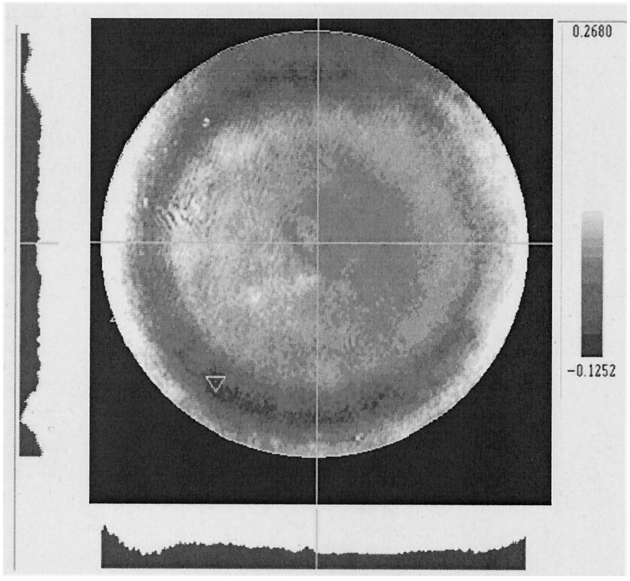

PV=0.3932λ, RMS=0.0425λ.

Fig. 9. Sample surface measurement of the test sphere. To reduce the random system noise, we averaged a collection of 146 such measurements to obtain results shown in Fig. 10.

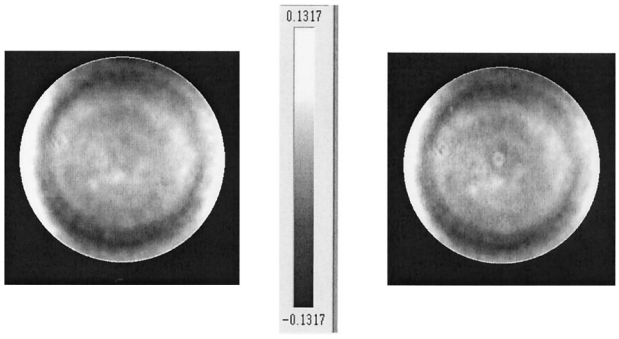

Fig. 10. Comparison of corrected measurement data. Left, 0.05542 cms wave-front, traditional method; right, 0.0489.2 rms wave-front, new CGH method.

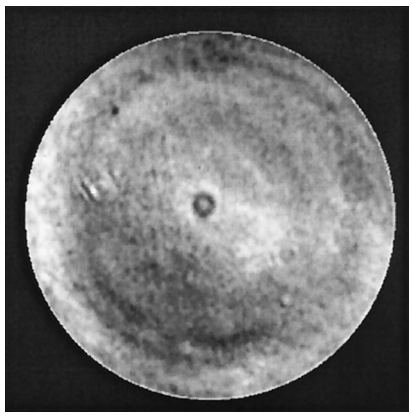

Fig. 11. Measurement difference when alignment marks are not used for the new method; rms wave-front error is 0.0116 λ.

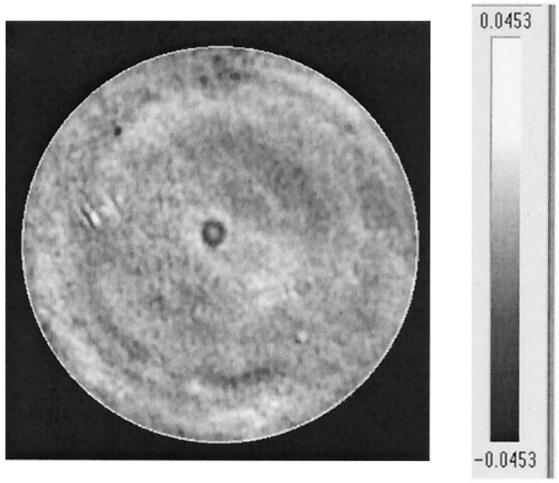

Fig. 12. Measurement difference (same as shown in Fig. 11) when lower-order coma and astigmatism are removed; rms wave-front error is 0.0069 λ.

slightly larger than the CGH, or roughly 20–35 mm for most cases. The last one, the wave-front error caused by the surface slope of the test plate (illumination side) appears to be very expensive to improve because its size has to match the test segment, which is 30 cm in this experiment and up to 2 m in other cases. A closer examination reveals that there is an inexpensive way to reduce this last error. Having the input beam and output beam of the test plate coaxial can greatly reduce this last error without imposing the tightened surface slope tolerance. This is accomplished with a beam splitter to separate the source and imaging sections.

C. Interferometer Repeatability

The repeatability of a test is an important performance gauge, as it shows how accurately does one measurement matches the next one. The repeatability is calculated by subtracting two consecutive measurements. For each of the measurements, tilt

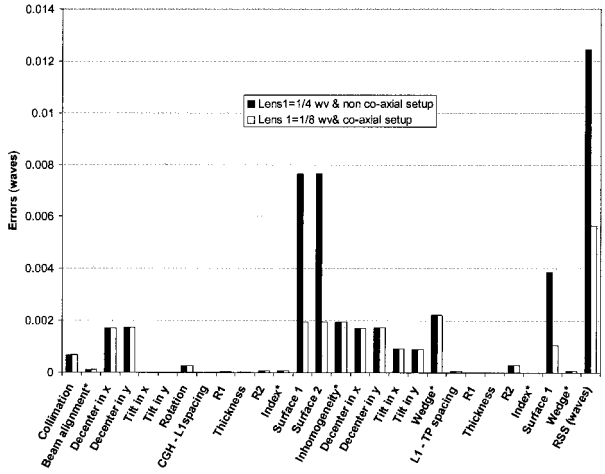

Fig. 13. Error budget for the as built system (λ/4 optics shows 0.0124-λ rms wave-front errors).

Table 9. Tolerance Analysis on the Projection Optics for the Experimental Setup[a]

Parameter	Value	Tolerance	Units	Tilt and Focus are Removed	
				λ/4 optics	λ/8 optics
Laser Beam					
Collimation	–	1	λ	0.000687	0.000687
Beam alignment*	–	0.007	deg	0.000119	0.000119
CGH					
Decenter in *x*	–	0.1	mm	0.0017	0.0017
Decenter in *y*	–	0.1	mm	0.0017	0.0017
Tilt in *x*	–	0.1	deg	0.0000	0.0000
Tilt in *y*	–	0.1	deg	0.0000	0.0000
Rotation	–	0.1	deg	0.0003	0.0003
CGH—L1 spacing	213.93	1	mm	0.000001	0.000001
Lens 1					
R1	206.335	0.1	mm	0.0001	0.0001
Thickness	6.15	0.1	mm	0.0000	0.0000
R2	−206.26	0.1	mm	0.0001	0.0001
Index	BK7	0.00001	–	0.0001	0.0001
Surface 1	Surf PV	0.25 or 0.125	λ	0.0076	0.0020
Surface 2	Surf PV	0.25 or 0.125	λ	0.0077	0.0020
Inhomogeneity	PV	2.00E-06	–	0.0020	0.0020
Decenter in *x*	–	0.1	mm	0.0017	0.0017
Decenter in *y*	–	0.1	mm	0.0017	0.0017
Tilt in *x*	–	0.1	mm	0.0009	0.0009
Tilt in *y*	–	0.1	mm	0.0009	0.0009
Wedge	–	8.73E-04	rad	0.0022	0.0022
L1–TP spacing	2908.38	1	mm	0.0001	0.0001
Test Plate					
R1	14222.5	2,000	m	0.0000	0.0000
Thickness	51.5366	0.0127	mm	0.0000	0.0000
R2	3998.4172	0.1	mm	0.0003	0.0003
Index	F. Silica	0.0001	–	0.0000	0.0000
Surface 1	Surf PV	0.125	λ	0.0038	0.0011
Wedge	–	7.27E-04	rad	0.0001	0.0001
Root Sum Squared (WF)	–	–	λ	0.0124	0.0056

[a]PV, peak-to-valley.

and focus are optimized to minimize the number of fringes across the CCD (i.e., the most fluffed-out fringes). Fig. 14 shows the result of subtracting two consecutive measurements. It shows that the rms noise is approximately 0.009λ (wave front).

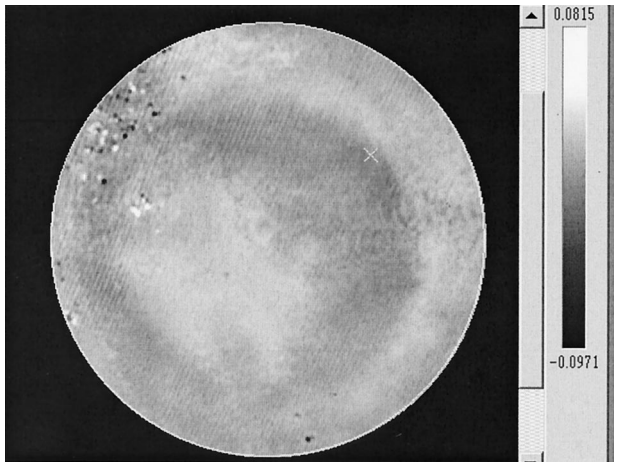

Fig. 14. Subtraction of two consecutive measurements showing typical rms test repeatability of 0.009 λ (wave front).

6. Conclusion

The results presented in this paper show that the new method of measuring off-axis aspherical segments with CGH and a test plate achieves excellent results. Documented in this paper is a complete case study that uses this innovative method for measuring 618 segments from a 30-m F/1 primary. The first-order proof-of-concept experiment shown here provides a compelling validation for this method's accuracy, repeatability, and cost effectiveness. Valuable lessons learned from this experiment provides a good launching pad for the next logic step, which is to carry this experiment one step further to test an off-axis asphere (currently in progress to be manufactured at the time of writing this paper).

Hardware used in the experiment was donated by the Rayleigh Optics and the computer generated hologram used in the experiment was fabricated and donated by A. Poleshchuk of Russian Academy of

Sciences. We thank Eugene Rudkevich of Taliescent Inc. for helpful editorial comments, Steve M. Arnold of Diffraction International for generous software assistance, and Cindy Gardner for assisting in manuscript preparation. This work has received funding from the National Aeronautics and Space Administration under contract #NGT5-50419, NOAO under contract #C10360A, and the Air Force Office of Scientific Research under contract #49620-02-1-0384.

References

1. J. Nelson, T. Mast, and S. Faber, "The design of the Keck Observatory and telescope," Keck Observatory Report 90 (W. M. Keck Library, Kamuela, Hawaii, 1985).
2. F. Pan, J. Burge, Y. Wang, and Z. Shan, "Fabrication and testing issues of segmented optics," Appl. Opt. **43,** 2632–2642 (2004).
3. F. Pan, "Measurement of aspherical surfaces using a test plate and computer generated holograms," Ph.D. dissertation (University of Arizona, Tucson, Ariz., 2002).
4. F. Pan and J. Burge, "Efficient testing of segmented aspherical mirrors by use of a reference plate and computer generated holograms: 1. Theory and system optimization," Appl. Opt. **43,** 5303–5312 (2004).
5. "Enabling a giant segmented mini telescope for the astronomical community (National Optical Astronomy Observatory, Tucson, Ariz., 24 May 2004), www.aura-nio.noao.edu/book/ch4.
6. F. Pan, J. Burge, "Design study for testing primary mirror segments from a a 30-m GSMT (Giant Segmented Mirror Telescope) using a test plate with computer generated holograms", a report submitted to the National Optical Astronomy Observatories, available at http://www.aura-nio.noao.edu/book/ch4/4.5.D.pdf.